Hall and Ohmic Heating Effects on the Peristaltic Transport of a Carreau–Yasuda Fluid in an Asymmetric Channel

Tasawar Hayat[a,c], Fahad M. Abbasi[a], Ahmed Alsaedi[b], and Fuad Alsaadi[c]

[a] Department of Mathematics, Quaid-I-Azam University 45320, Islamabad 44000, Pakistan
[b] Nonlinear Analysis and Applied Mathematics (NAAM) Research Group, Faculty of Science, King Abdulaziz University, Jeddah 21589, Saudi Arabia
[c] Department of Electrical and Computer Engineering, Faculty of Engineering, King Abdulaziz University, Saudi Arabia

Reprint requests to F. M. A.; E-mail: abbasisarkar@gmail.com

Z. Naturforsch. **69a,** 43 – 51 (2014) / DOI: 10.5560/ZNA.2013-0074
Received May 22, 2013 / revised September 13, 2013 / published online December 18, 2013

The effects of Hall current and Ohmic heating are analyzed for the peristaltic flow of a Carreau–Yasuda fluid in an asymmetric channel. The mathematical model for peristalsis of the Carreau–Yasuda fluid is provided for the first time in the literature. The problem is developed in the presence of viscous dissipation. Solutions for pressure gradient, stream function, axial velocity, and temperature are established and discussed. The heat transfer rate at the wall is first computed numerically and then examined. A comparative study for viscous, Carreau, and Carreau–Yasuda fluids is also made.

Key words: Mathematical Modelling; Carreau–Yasuda Fluid; Ohmic Heating; Hall Effects.

1. Introduction

Investigations related to peristaltic mechanism have a key importance in physiological and industrial processes. In biological process, such mechanism is obvious in esophageal transport, earthworm mobility, gastrointestinal tract, urine transport, spermatozoa transport, blood circulation in vessels etc. The peristaltic pumps are especially useful in the environmental, medical, and pharmaceutical applications. These applications include DNA analysis, drug delivery and chemical/biological agent detection sensors on microchips [1]. No doubt, the movements of biological fluids or solutes in such applications are controlled electrically. This activity generates the effect of Joule heating. In particular the flow of electrically conducting fluids is of great value in shock tubes, pumps, and flow meters, accelerators, and magnetohydrodynamic generators. The flows in many devices of this kind are subjected by heat either that dissipated internally through viscous or Joule heating or that resulted because of electric currents in the walls. Hence there are several existing studies of peristalsis of electrically conducting fluids in the presence/absence of heat transfer effects (see few recent publications [2 – 10] and the references therein.).

Although the peristaltic flow of electrically conducting fluid is paid due attention but such flow with Hall and Ohmic heating effects is not properly attended. In an earlier work, Hayat et al. [11] discussed the peristaltic flow of a Maxwell fluid. Here an incompressible Maxwell fluid fills the porous medium. The peristaltic transport of particle-fluid suspension in the presence of Hall current is examined by Gad [12]. Blood flow through a stenotic artery in presence of Hall effect is analyzed by Mekheimer and El Kot [13]. The blood in this study is characterized by constitutive equations of micropolar fluid. The Hall parameter in such analysis is in fact the ratio of electron-cyclotron frequency and the electron-atom collision frequency. This effect can alter the results considerably when the applied magnetic field is strong or when the collision frequency is low. In dealing with weak and moderate magnetic fields, the Hall effect is ignored and the results give good agreement with experimental data. However, when dealing with strong magnetic fields then the Hall current is important as it has a considerable effect on the current density and consequently on the Lorentz force term. These facts make the impact of Hall current on the flow worth studying.

To the best of our knowledge, no study is available on the peristaltic transport of a Carreau–Yasuda fluid.

Carreau–Yasuda is a five constant model which can explain fluid rheology in a better way than power law or Carreau model. As a special case it can be reduced into Carreau or even Newtonian model. This model has the tendency of predicting shear thinning behaviour in its limiting case. With these motivations, this study deals with the peristaltic transport of a Carreau–Yasuda fluid with Hall effects. Analysis of heat transfer with viscous dissipation and Ohmic heating is made. The problem is modelled under long wavelength and low Reynolds number approximation. The resulting nonlinear equations are solved numerically. Results are analyzed through graphs and tables at the end. Results for viscous and Carreau fluids are also recovered. It is shown that the problem of peristaltic transport with hydrodynamic (HD) and magnetohydrodynamic (MHD) can be obtained as the special cases. The impact of several parameters on the flow quantities are plotted and discussed. The key findings of this study are summarized at the end.

2. Methods

2.1. Mathematical Analysis

We consider the flow of an incompressible Carreau–Yasuda fluid in a two-dimensional asymmetric channel of width $d_1 + d_2$. The flow in the channel is generated due to sinusoidal wave trains propagating along the channel walls with constant wave speed c. The asymmetry here is because of the wave trains along the channel walls have different amplitudes and phases. The geometry of wall surfaces is defined as

$$\begin{aligned} &\overline{H}_1(\overline{X},\bar{t}) = \overline{d}_1 + \overline{\varepsilon}_1 \ \text{(upper wall) and} \\ &\overline{H}_2(\overline{X},\bar{t}) = -\left(\overline{d}_2 + \overline{\varepsilon}_2\right) \ \text{(lower wall),} \end{aligned} \tag{1}$$

where ε_1 and ε_2 are the disturbances produced due to propagation of peristaltic waves along upper and lower walls, respectively. The disturbances are of the forms

$$\begin{aligned} \overline{\varepsilon}_1 &= \overline{a}_1 \cos\left(\frac{2\pi}{\lambda}(\overline{X} - c\bar{t})\right), \\ \overline{\varepsilon}_2 &= \overline{a}_2 \cos\left(\frac{2\pi}{\lambda}(\overline{X} - c\bar{t}) + \gamma\right), \end{aligned} \tag{2}$$

where $\overline{a}_1$, $\overline{a}_2$ are the amplitudes of the waves, γ $(0 \leq \gamma \leq \pi)$ is the phase difference, t is the time, λ is the wavelength, and $\overline{X}$ and $\overline{Y}$ are the rectangular coordinates with $\overline{X}$ measured along the channel length and $\overline{Y}$ normal to $\overline{X}$. It is important to mention that $\gamma = 0$ and $\gamma = \pi$ correspond to the cases where the channel is symmetric with waves out of phase and waves in phase, respectively. Moreover $\overline{a}_1$, $\overline{a}_2, \overline{d}_1, \overline{d}_2$, and γ satisfy the condition

$$\overline{d}_1^2 + \overline{d}_2^2 + 2\overline{a}_1\overline{a}_2\cos\gamma \leq \left(\overline{d}_1 + \overline{d}_2\right)^2.$$

The fluid is electrically conducting in the presence of an uniform applied magnetic field $(0, 0, B_0)$. Electric and induced magnetic field effects are not taken into account. However the influence of the Hall current is considered. The generalized Ohms' law for Hall effects is given by

$$\overline{J} = \sigma\left[\overline{E} + \overline{V} \times \overline{B}\right] - \frac{\sigma}{e\, n_{\mathrm{e}}}\left[\overline{J} \times \overline{B}\right]. \tag{3}$$

In above expression, $\overline{J}$ denotes the current density, $\overline{V}$ the velocity, e the electron charge, n_{e} the number density of electrons, and σ the electric conductivity of the fluid. The present flow situation is governed by Maxwell's equations, generalized Ohms' law, and the following equations:

$$\overline{\nabla} \cdot \overline{V} = 0, \tag{4}$$

$$\rho \frac{\mathrm{d}\overline{V}}{\mathrm{d}\bar{t}} = \overline{\nabla}\overline{p} + \overline{\nabla} \cdot \overline{\tau} + \overline{J} \times \overline{B}, \tag{5}$$

$$\rho C_p \frac{\mathrm{d}T}{\mathrm{d}\bar{t}} = K\left[\frac{\partial T^2}{\partial \overline{X}^2} + \frac{\partial T^2}{\partial \overline{Y}^2}\right] + \overline{\Phi} + \overline{\Phi}_1, \tag{6}$$

where $\overline{V} = \left[\overline{U}(\overline{X}, \overline{Y}, \bar{t}), \overline{V}(\overline{X}, \overline{Y}, \bar{t}), 0\right]$ is the velocity field, $\overline{p}$ the pressure, $\overline{\tau}$ the extra stress tensor, ρ the fluid density, C_p the specific heat, T the fluid temperature, K the thermal conductivity, $\overline{\Phi}$ the viscous dissipation, $\overline{\Phi}_1$ the Ohmic heating term, and $\bar{t}$ the time.

2.2. Stress Tensor for Carreau–Yasuda Fluid

The constitutive equation for Carreau–Yasuda fluid is given by [14 – 17]

$$\overline{\tau} = \mu(\dot{\gamma})\overline{A}_1, \tag{7}$$

where A_1 is the first Rivlin Erickson tensor, and the apparent fluid viscosity $\mu(\dot{\gamma})$ is given by

$$\mu(\dot{\gamma}) = \mu_\infty + (\mu_0 - \mu_\infty)\left[1 + (\Gamma\dot{\gamma})^a\right]^{\frac{n-1}{a}}. \tag{8}$$

In above relation μ_∞ is the infinite shear-rate viscosity, μ_0 the zero shear-rate viscosity, n the dimensionless

power law index, Γ and a are the fluid parameters. $\dot{\gamma}$ is defined by

$$\dot{\gamma} = \sqrt{\frac{1}{2}\sum\sum \dot{\gamma}_{ij}\dot{\gamma}_{ij}} = \sqrt{\frac{1}{2}\prod},$$

where $\prod$ is the second invariant of the strain-rate tensor. This fluid model is a generalization of the viscous model and predicts more precisely the variation of viscosity μ with shear rate than the power law rheological model. One of the major advantages of this fluid model is that it involves five parameters to describe the rheology of the fluid when compared with two parameters of the power law model. This model predicts the shear thinning case when $n < 1$ and shear thickening effect for $n > 1$. We consider here the case for $\mu_\infty = 0$ and thus

$$\mu(\dot{\gamma}) = \mu_0 \left[1 + (\Gamma\dot{\gamma})^a\right]^{\frac{n-1}{a}}.$$

It is worth mentioning here that this model reduces to the Carreau fluid model for $a = 2$ and to the viscous fluid model when either $\Gamma = 0$ or $n = 1$.

2.3. Transformation and Simplification of the Problem

Note that the flow equations in the laboratory frame are time dependent. However if we choose a wave frame which is moving along the wave with the same speed then it can be treated steady. The transformations between laboratory and wave frames are related as follows:

$$\begin{aligned} &\overline{x} = \overline{X} - c\overline{t}\,,\ \overline{y} = \overline{Y}\,,\ \overline{u} = \overline{U} - c\,,\\ &\overline{v} = \overline{V}\,,\ \overline{p}(\overline{x},\overline{y}) = \overline{P}(\overline{X},\overline{Y},\overline{t})\,, \end{aligned} \tag{9}$$

where $(\overline{u},\overline{v})$ and $\overline{p}$ are the velocity components and pressure in the wave frame, while $(\overline{U},\overline{V})$ and $\overline{P}$ are the velocity components and pressure in the laboratory frame. The equations in the wave frame are given by

$$\frac{\partial\overline{u}}{\partial\overline{x}} + \frac{\partial\overline{v}}{\partial\overline{y}} = 0, \tag{10}$$

$$\begin{aligned} &\rho\left((\overline{u}+c)\frac{\partial}{\partial\overline{x}} + \overline{v}\frac{\partial}{\partial\overline{y}}\right)(\overline{u}+c) = -\frac{\partial\overline{p}}{\partial\overline{x}} + \frac{\partial\overline{\tau}_{\overline{x}\overline{x}}}{\partial\overline{x}}\\ &+ \frac{\partial\overline{\tau}_{\overline{x}\overline{y}}}{\partial\overline{y}} - \frac{\sigma B_0^2}{1+m^2}\left((\overline{u}+c) - m\overline{v}\right), \end{aligned} \tag{11}$$

$$\begin{aligned} &\rho\left((\overline{u}+c)\frac{\partial}{\partial\overline{x}} + \overline{v}\frac{\partial}{\partial\overline{y}}\right)\overline{v} = -\frac{\partial\overline{p}}{\partial\overline{y}} + \frac{\partial\overline{\tau}_{\overline{y}\overline{x}}}{\partial\overline{x}}\\ &+ \frac{\partial\overline{\tau}_{\overline{y}\overline{y}}}{\partial\overline{y}} + \frac{\sigma B_0^2}{1+m^2}\left(m(\overline{u}+c) + \overline{v}\right), \end{aligned} \tag{12}$$

$$\begin{aligned} &\rho C_p\left((\overline{u}+c)\frac{\partial T}{\partial\overline{x}} + \overline{v}\frac{\partial T}{\partial\overline{y}}\right) = K\left[\frac{\partial^2 T}{\partial\overline{x}^2} + \frac{\partial^2 T}{\partial\overline{x}^2}\right]\\ &+ \upsilon\Phi + \frac{\sigma B_0^2}{1+m^2}\left((\overline{u}+c)^2 + \overline{v}^2\right). \end{aligned} \tag{13}$$

Here $m = \sigma B_0^2/e n_e$ is the Hall parameter, and the stress components are given by

$$\begin{aligned} \overline{\tau}_{\overline{x}\overline{x}} &= 2\mu_0\left[1 + \frac{n-1}{a}\Gamma^a\left\{2\overline{u}_x^2 + 2\overline{v}_y^2 + (\overline{u}_y + \overline{v}_x)^2\right\}^{\frac{a}{2}}\right]\\ &\cdot\overline{u}_x\,,\\ \overline{\tau}_{\overline{x}\overline{y}} &= \mu_0\left[1 + \frac{n-1}{a}\Gamma^a\left\{2\overline{u}_x^2 + 2\overline{v}_y^2 + (\overline{u}_y + \overline{v}_x)^2\right\}^{\frac{a}{2}}\right]\\ &\cdot(\overline{u}_y + \overline{v}_x)\,,\\ \overline{\tau}_{\overline{y}\overline{y}} &= 2\mu_0\left[1 + \frac{n-1}{a}\Gamma^a\left\{2\overline{u}_x^2 + 2\overline{v}_y^2 + (\overline{u}_y + \overline{v}_x)^2\right\}^{\frac{a}{2}}\right]\\ &\cdot\overline{v}_y\,. \end{aligned} \tag{14}$$

Now defining the following dimensionless quantities:

$$\begin{aligned} &x = \frac{\overline{x}}{\lambda},\ y = \frac{\overline{y}}{d_1},\ u = \frac{\overline{u}}{c},\ v = \frac{\overline{v}}{c\delta},\ \delta = \frac{d_1}{\lambda},\\ &h_1 = \frac{\overline{H}_1}{d_1},\ h_2 = \frac{\overline{H}_2}{d_1},\ d = \frac{d_2}{d_1},\ b_1 = \frac{a_1}{d_1},\ b_2 = \frac{a_2}{d_1},\\ &p = \frac{d_1^2\overline{p}}{c\lambda\mu_0},\ \mathrm{Re} = \frac{\rho c d_1}{\mu_0},\ t = \frac{c\overline{t}}{\lambda},\ \theta = \frac{T - T_0}{T_1 - T_0},\\ &\tau = \frac{d_1\overline{\tau}}{\mu_0 c},\ \mathrm{Br} = \mathrm{Pr}E,\ E = \frac{c^2}{C_p(T_1 - T_0)},\\ &\mathrm{Pr} = \frac{\mu_0 C_p}{K},\ M^2 = \left(\frac{\sigma}{\mu_0}\right)B_0^2 d_1^2,\ \mathrm{We} = \frac{\Gamma c}{d_1},\\ &\varphi = \frac{1}{1+m^2},\ u = \psi_y,\ v = -\psi_x\,. \end{aligned} \tag{15}$$

Making use of long wavelength and low Reynolds number approximations [7, 10, 18 – 20], we have

$$\begin{aligned} \frac{\partial p}{\partial x} &= \frac{\partial}{\partial y}\left[1 + \frac{n-1}{a}\mathrm{We}^a\left(\frac{\partial^2\psi}{\partial y^2}\right)^a\right]\frac{\partial^2\psi}{\partial y^2}\\ &+ M^2\varphi\left(\frac{\partial\psi}{\partial y} + 1\right), \end{aligned} \tag{16}$$

$$0 = \frac{\partial p}{\partial y}, \tag{17}$$

$$0=\frac{\partial^2\theta}{\partial y^2}+\mathrm{Br}\left[1+\frac{n-1}{a}\mathrm{We}^a\left(\frac{\partial^2\psi}{\partial y^2}\right)^a\right]\cdot\left(\frac{\partial^2\psi}{\partial y^2}\right)^2+\mathrm{Br}M^2\varphi\left(\frac{\partial\psi}{\partial y}+1\right)^2, \tag{18}$$

where Re is the Reynolds number, θ the dimensionless temperature, T_0, T_1 the temperatures at the upper and lower walls, Br the Brinkman number, Pr the Prandtl number, E the Eckert number, M the Hartman number, We the Weissenberg number, and ψ the stream function. Further, the continuity equation is identically satisfied and (16) and (17) give

$$0=\frac{\partial^2}{\partial y^2}\left[1+\frac{n-1}{a}\mathrm{We}^a\left(\frac{\partial^2\psi}{\partial y^2}\right)^a\right]\frac{\partial^2\psi}{\partial y^2}+M^2\varphi\left(\frac{\partial^2\psi}{\partial y^2}\right). \tag{19}$$

From (17), we have $p\neq p(y)$. The volume flow rate in laboratory frame is given by

$$Q=\int_{H_2}^{H_1}\overline{U}\left(\overline{X},\overline{Y},\bar{t}\right)\,\mathrm{d}\overline{Y}, \tag{20}$$

where $H_{1,2}$ are functions of $\overline{X}$ and $\bar{t}$. The above equation in the wave frame becomes

$$q=\int_{h_2}^{h_1}\overline{u}\left(\bar{x},\bar{y}\right)\,\mathrm{d}\bar{y}. \tag{21}$$

The mean flow rate (averaged flow) over a period T_f at fixed position $\overline{X}$ is defined as

$$\overline{Q}=\int_0^{T_\mathrm{f}}Q\,\mathrm{d}t. \tag{22}$$

Defining the dimensionless mean flow rate η in the laboratory frame and F in the wave frame by

$$\eta=\frac{\overline{Q}}{cd_1},\quad F=\frac{q}{cd_1}, \tag{23}$$

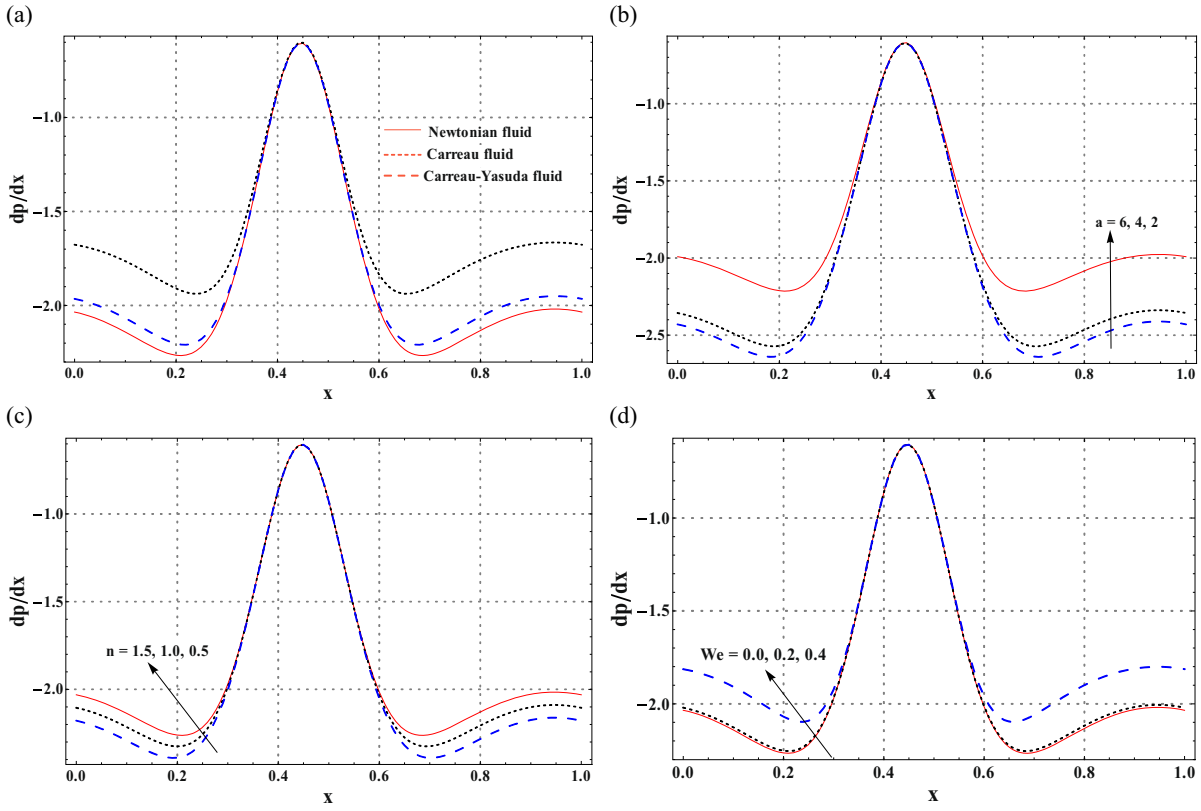

Fig. 1 (colour online). Effects of various parameters on the pressure gradient $\mathrm{d}p/\mathrm{d}x$ when $\mathrm{We}=0.3$, $M=1.5$, $\phi=0.5$, $\mathrm{Br}=0.3$, $b_1=0.4$, $b_2=0.3$, $\gamma=\pi/4$, $d=0.7$, and $\eta=0.7$. (a) different fluid models, (b) non-Newtonian parameter a, (c) non-Newtonian parameter n, (d) Weissenberg number We.

we have

$$\eta = F + 1 + d\,, \tag{24}$$

$$F = \int_{h_2(x)}^{h_1(x)} \frac{\partial \psi}{\partial y}\,\mathrm{d}\bar{y} = \psi(h_1) - \psi(h_2)\,,$$

$$h_1 = 1 + b_1 \cos 2\pi x\,, \text{ and}$$

$$h_2 = -d - b_2 \cos(2\pi x + \gamma)\,.$$

The dimensionless boundary conditions are

$$\psi = F/2 \text{ at } y = h_1 \text{ and}$$

$$\psi = -F/2 \text{ at } y = h_2\,, \tag{25}$$

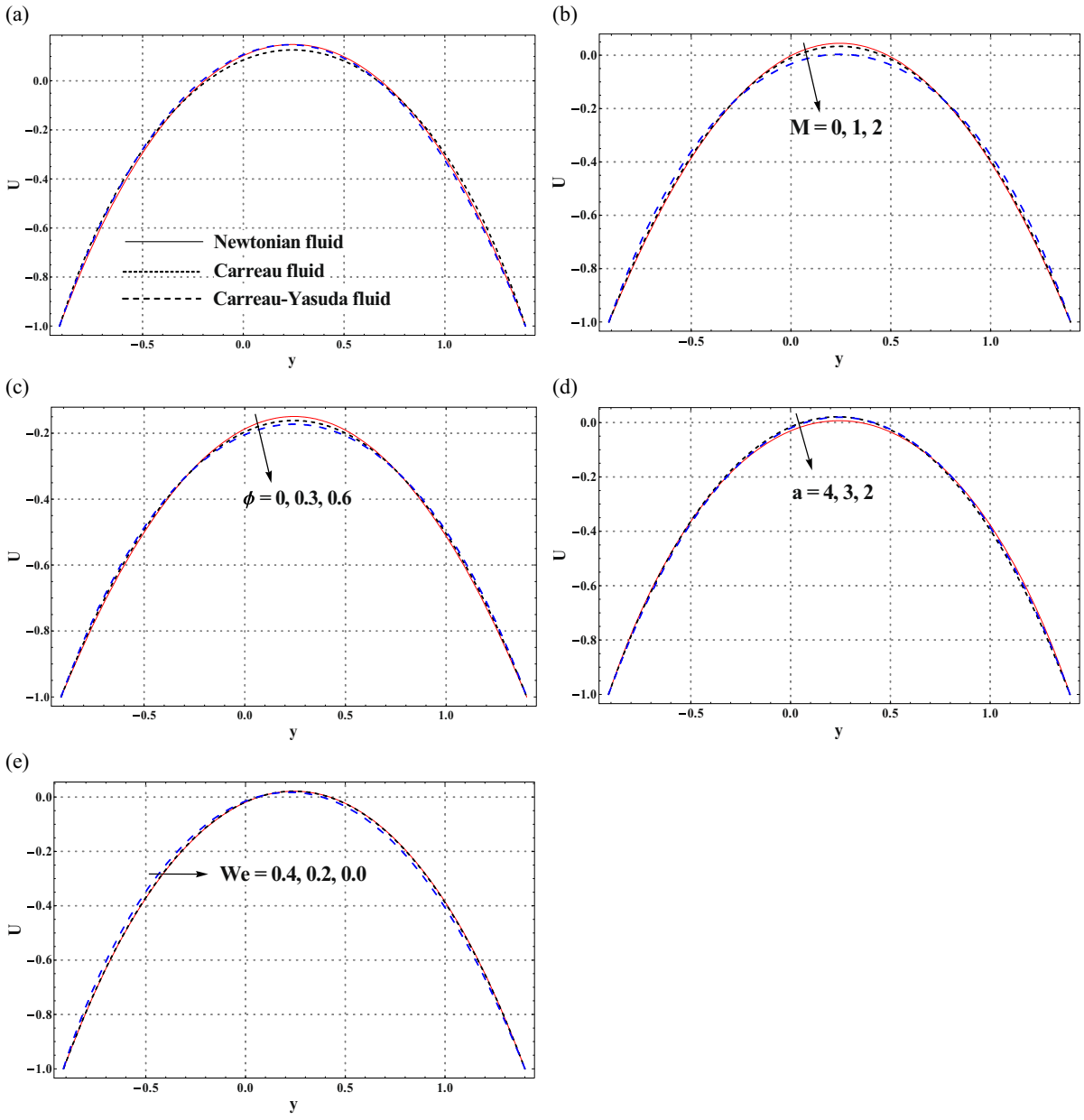

Fig. 2 (colour online). Variation of axial velocity subject to different parameters when $n = 0.5$, Br $= 0.3$, $b_1 = 0.4$, $b_2 = 0.3$, $\gamma = \pi/4$, $d = 0.7$, $\eta = 0.7$, and $x = 0$. (a) different fluid models, (b) Harman number M, (c) Hall parameter ϕ, (d) non-Newtonian parameter a, (e) Weissenberg number We .

$$\frac{\partial \tau}{\partial y} = -1 \text{ at } y = h_1 \text{ and } y = h_2, \tag{26}$$

$$\theta = 0 \text{ at } y = h_1 \text{ and } \theta = 1 \text{ at } y = h_2. \tag{27}$$

2.4. Solution Procedure

Here our intention is to solve the nonlinear flow problem numerically. Hence we have used the built-in numerical technique for solving our problem making use of the software Mathematica. The chosen unit step size for the variations is 0.01 which obviously can be varied. The relevant graphs and tables are prepared.

Table 1. Heat transfer rate at the upper wall $(-\theta'(h_1))$ for different fluid models when $n = 0.5$, $b_1 = 0.4$, $b_2 = 0.3$, $\gamma = \pi/4$, $d = 0.7$, $\eta = 0.7$, and $\mathrm{Br} = 0.3$.

x	Newtonian	Carreau	Carreau–Yasuda
0.0	1.0370	1.0085	1.0362
0.25	1.0955	1.0618	1.0947
0.5	1.1281	1.1838	1.1560

3. Results

Plots for pressure gradient (Fig. 1a – d), axial velocity (Fig. 2a – e), and temperature (Fig. 3a – d) are an-

Table 2. Heat transfer rate at the upper wall $(-\theta'(h_1))$ for different cases of applied magnetic field when $n = 0.5$, $M = 1.5$, $\phi = 0.5$, $\mathrm{Br} = 0.3$, $b_1 = 0.4$, $b_2 = 0.3$, $\gamma = \pi/4$, $d = 0.7$, and $\eta = 0.7$.

x	HD	MHD	MHD with Hall effects
0.0	0.8091	1.2573	1.0347
0.25	1.0081	1.1753	1.0920
0.5	1.1575	1.1407	1.1572

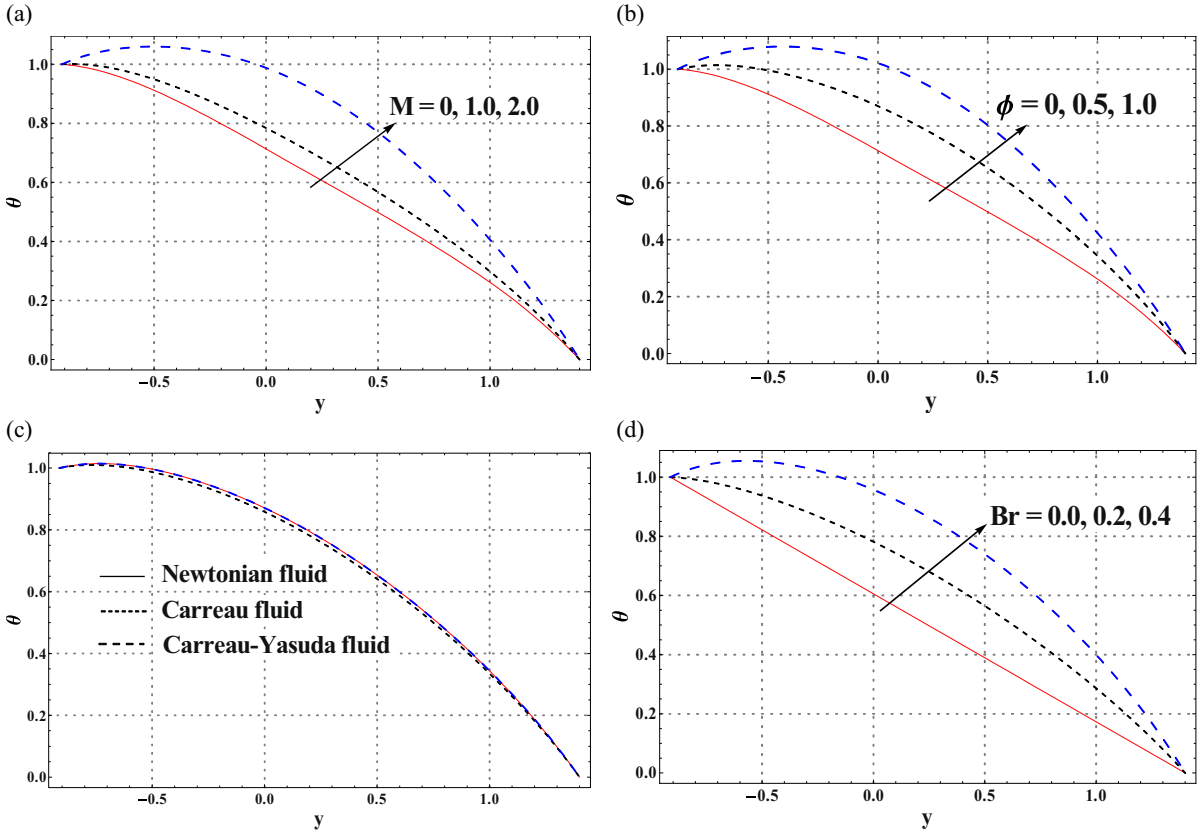

Fig. 3 (colour online). Variation in temperature for the different parameters when $n = 0.5$, $b_1 = 0.4$, $b_2 = 0.3$, $\gamma = \pi/4$, $d = 0.7$, $\eta = 0.7$, and $x = 0$. (a) Harman number M, (b) Hall parameter ϕ, (c) different fluid models, (d) Brinkman number Br.

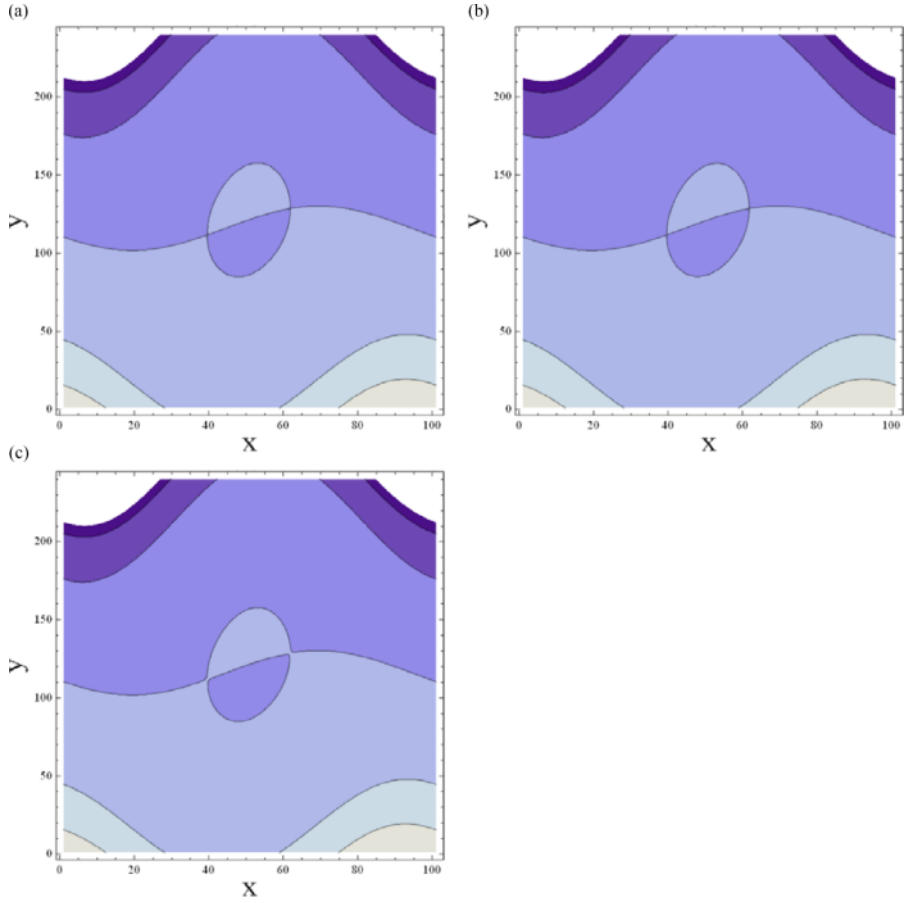

Fig. 4 (colour online). Streamlines for different fluid models when $n = 0.5$, $b_1 = 0.4$, $b_2 = 0.3$, $\gamma = \pi/4$, $d = 0.7$, $\eta = 0.7$, and $\mathrm{Br} = 0.3$. (a) Newtonian fluid, (b) Carreau fluid, and (c) Carreau–Yasuda fluid.

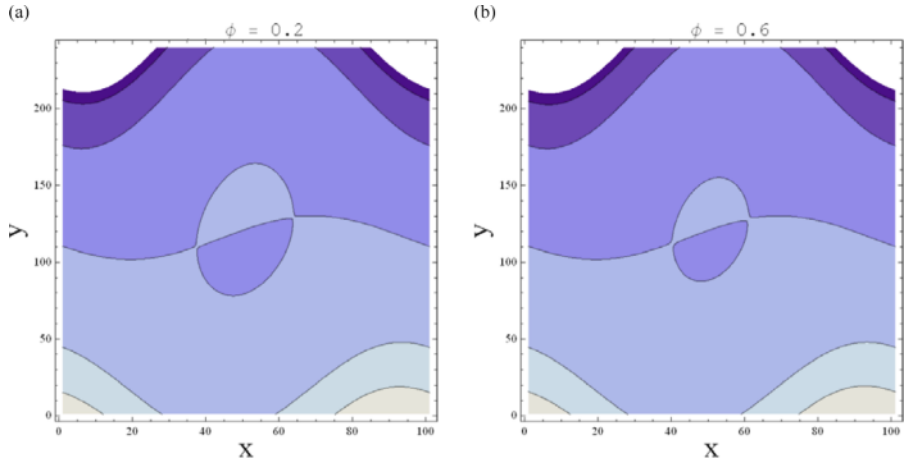

Fig. 5 (colour online). Streamlines for variation in Hall parameter ϕ, when $n = 0.5$, $b_1 = 0.4$, $b_2 = 0.3$, $\gamma = \pi/4$, $d = 0.7$, $\eta = 0.7$, and $\mathrm{Br} = 0.3$.

alyzed. Numerical values of the heat transfer rate at the upper wall for different values of pertinent parameters and variation in x are presented in Tables 1 and 2.

3.1. Analysis of Pressure Gradient

It is found that the pressure gradient has an oscillatory characteristic. This is due to peristalsis. Figure 1a shows the pressure gradient for a viscous fluid (We $= 0$ or $n = 1$), a Carreau fluid ($a = 2$), and a Carreau–Yasuda fluid. This figure shows that the Carreau fluid has a higher value of pressure gradient when compared with the other fluids. The pressure gradient is minimal for a viscous fluid. The pressure gradient also decreases when the non-Newtonian parameter a is increased. Such decrease is more prominent when a varied between 2 and 4 (see Fig. 1b). The shear thickening ($n > 1$) fluid has a smaller value of pressure gradient when compared with shear thinning fluid ($n < 1$) (see Fig. 1c). Figure 1d depicts that an increase in Weissenberg number increases the pressure gradient. This shows that the pressure gradient increases due to large non-Newtonian characteristics.

3.2. Study of Axial Velocity

The axial velocity traces a parabolic trajectory with a maximum value occurring near the center of the channel. Figure 2a shows that the maximum value of velocity for a Carreau fluid is less than the velocity of viscous or Carreau–Yasuda fluid. The velocity profile of a non-Newtonian fluid flattens near the center of the channel as expected for a shear thinning fluid. Increasing the value of the non-Newtonian parameter We disturbs the symmetry of the velocity plots about the center of the channel (see Fig. 2e). The maximum value of the velocity tends to shift towards the lower wall when a higher value is assigned to We. All these results are qualitatively in good agreement with the theoretical and experimental findings of Gijsen et al. [16, 17]. An increase in the intensity of the applied magnetic field decreases the velocity (see Fig. 2b). Setting $\varphi = \frac{1}{1+m^2}$, we note that φ can neither be negative nor it can be greater than 1. Here $\varphi = 0$ or $M = 0$ corresponds to the case of a hydrodynamic fluid. Figure 2c shows that an increase in φ decreases the maximum value of the velocity. An increase in value of a increases the value of the axial velocity (see Fig. 2d).

3.3. Heat Transfer Analysis

The dimensionless temperature is examined through Figure 3a – d. As we have taken into account the Ohmic heating effect, so the applied magnetic field largely affects the temperature of the fluid. The temperature increases with an increase in Hartman number. Similarly, an increase in the Hall parameter φ increases the temperature (see Fig. 3a,b). Figure 3c shows that the Carreau fluid has a temperature less than that of a viscous or a Carreau–Yasuda fluid. Moreover, the Brinkman number has large impact on the fluid temperature. Increase in Br increases the fluid temperature by a considerable amount (see Fig. 3d). An analysis of streamlines is presented in Figs. 4 and 5. They show that the size of the trapped bolus is smaller for a Carreau–Yasuda fluid. Moreover, symmetry of the bolus about the centerline is not intact for the Carreau–Yasuda fluid. An increase in the value of φ largely reduces the bolus size.

Some numerical values of heat transfer rate at the upper wall are given in Table 1 for different fluid models and in Table 2 for various cases of MHD. It is observed that as the value of x increases, the heat transfer rate gains a higher value. A Carreau fluid has a smaller heat transfer rate when compared with a Carreau–Yasuda fluid. On the other hand, the value of heat transfer rate grows rapidly with x for the Carreau fluid. The heat transfer rate in the absence of a magnetic field is small and it increases in the presence of an applied magnetic field. The heat transfer rate is small for the case when we consider Hall effects through φ.

4. Concluding Remarks

Hall and Ohmic heating effects on the peristaltic transport of a Carreau–Yasuda fluid in an asymmetric channel are studied in this communication. Key findings of present analysis are summarized below:

- A Carreau fluid possesses higher value of pressure gradient when compared with the Carreau–Yasuda and Newtonian fluid.
- The velocity is a decreasing function of Hall parameter and Hartman number whereas it is an increasing function of the non-Newtonian parameter a.
- Hartman number and Hall parameter have an increasing effect on the temperature.

- The temperature of the Carreau fluid is less than that of viscous or Carreau–Yasuda fluid.
- The size of the trapped bolus decreases with an increase in the Hall parameter.
- The heat transfer rate at the wall is higher for a MHD fluid but it decreases when Hall effects are taken into account.

Acknowledgement

We are grateful to the reviewers for their useful suggestions. This paper was funded by the Deanship of Scientific Research (DSR), King Abdulaziz University, Jeddah, under Grant no. 8-135/1434HiCi. The authors, therefore, acknowledge with thanks DSR technical and financial support.

[1] G. Karniadakis, A. Beskok, and N. Aluru, Microflows and Nanonflows, Springer 2005.
[2] Kh. S. Mekheimer, Phys. Lett. A **372**, 4271 (2008).
[3] M. Kothandapani and S. Srinivas, Int. J. Nonlin. Mech. **43**, 915 (2008).
[4] N. Ali, T. Hayat, and Y. Wang, Int. J. Numer. Meth. Fluids **64**, 992 (2010).
[5] S. K. Pandey and D. Tripathi, Z. Naturforsch. **66a**, 172 (2011).
[6] F. M. Abbasi, T. Hayat, A. Alsaedi, and B. Ahmed, Appl. Math. Inf. Sci. **8**, 211 (2014).
[7] S. Nadeem, N. S. Akbar, and T. Hayat, Z. Naturforsch. **65a**, 901 (2010).
[8] S. Srinivas and M. Kothandapani, Appl. Math. Comp. **213**, 197 (2009).
[9] T. Hayat and S. Hina, Nonlin. Anal.: Real World Appl. **11**, 3155 (2010).
[10] T. Hayat, F. M. Abbasi, and S. Obaidat, Magnetohydrodynamics **47**, 295 (2011).
[11] T. Hayat, N. Ali, and S. Asghar, Phys. Lett. A **363**, 397 (2007).
[12] N. S. Gad, Appl. Math. Comput. **217**, 4313 (2011).
[13] Kh.S. Mekheimer and M. A. El Kot, Appl. Math. Mech. **29**, 1093 (2008).
[14] L. C. F. Andrade, J. A. Petronílio, C. E. de A. Maneschy, and D. O. de A. Cruz, J. Braz. Soc. Mech. Sci. Eng. **29**, 162 (2007).
[15] A. Pinarbasi and A. Liakopoulos, J. Non-Newtonian Fluid Mech. **57**, 227 (1995).
[16] F. J. H. Gijsen, F. N. van de Vosse, and J. D. Janssen, J. Biomech. **32**, 601 (1999).
[17] F. J. H. Gijsen, E. Allanic, F. N. van de Vosse, and J. D. Janssen, J. Biomech. **32**, 705 (1999).
[18] A. H. Shapiro, M. Y. Jaffrin, and S. L. Wienberg, J. Fluid Mech. **37**, 799 (1969).
[19] T. Hayat, H. Yasmin, M. S. Alhuthali, and M. A. Kutbi, J. Mech. **29**, 599 (2013).
[20] M. Mustafa, S. Hina, T. Hayat, and A. Alsaedi, Int. J. Heat Mass Trans. **55**, 4871 (2012).